Balaena ricei, a New Species of Bowhead Whale from the Yorktown Formation (Pliocene) of Hampton, Virginia

James W. Westgate and Frank C. Whitmore, Jr.

ABSTRACT

Fossil species of *Balaena* have previously been named on the basis of material from the Western Hemisphere, but all are founded upon undiagnostic material. The holotype of *B. ricei* new species consists of a partial skull, partial mandible, all major flipper bones, and representatives of all types of vertebrae, allowing comparison with the two best-known European species.

This study, together with the known occurrence of *Balaena* species in the Pliocene of Europe, strengthens the conclusion that bowhead whales were present on both sides of the North Atlantic Ocean at that time. By contrast, remains of *Balaena* have not been reported from Miocene deposits of the Atlantic coast of North America.

Introduction

In September 1960 William Rice discovered the skull and skeleton of a large bowhead whale while excavating materials from his borrow pit in Hampton, Virginia (Figure 1). This was the first recorded occurrence of a bowhead whale from the Yorktown Formation (U.S. Geological Survey, 1962, 1965). Another bowhead whale was found in 1985 at the old Hampton Landfill on Magruder Boulevard (G.H. Johnson, pers. comm., 1985). It consists of a set of fused cervical vertebrae, two mandibles, the rib cage, six dorsal vertebrae, and both scapulae, ulnae, and radii. The specimen, of late Yorktown age, is in the collections of the Department of Geology, College of William and Mary, Williamsburg, Virginia.

The family Balaenidae, the bowhead and right whales, has a narrow, highly arched rostrum and fused cervical vertebrae that

James W. Westgate, Department of Geology, Lamar University, Beaumont, Texas 77710. Frank C. Whitmore, Jr., Research Associate, Department of Paleobiology, National Museum of Natural History, Smithsonian Institution, Washington, D.C. 20560-0121.

allow ready identification of the members of the family; both characters are seen in the present specimen. The fossil record of the family goes back to the earliest Miocene (McLeod et al., 1993), but the record is sparse until the late Miocene and the Pliocene, when fossil occurrences indicate widespread, perhaps global, distribution of balaenids. Despite the wide distribution of the family, its generic and specific diversity have always been low. Today the family is represented by two monotypic genera: *Eubalaena,* the right whale, and *Balaena,* the bowhead. Several extinct genera of Balaenidae have been described, but only one, *Balaenula* Van Beneden (1872), is now generally accepted.

The specimen described differs from *Eubalaena* in having a larger head, whose profile has a continuous curve from the occipital condyles to the anterior end of the rostrum, and in possessing a coracoid process on the scapula (True, 1904; McLeod et al., 1993). It differs from *Balaenula* in its greater size.

Many fossil species have been described and assigned to the genus *Balaena.* Most of these were published in the nineteenth century, and many are based upon undiagnostic material. Of the many nominal species, McLeod et al. (1993) recognized four as valid species of *Balaena: B. affinis* Owen, 1844; *B. etrusca* Capellini, 1873; *B. montalionis* Capellini, 1904; and *B. primigenias* Van Beneden, 1872.

In modern times, bowhead whales lived in great numbers along the Atlantic coast of North America. In spite of this, no balaenid remains have yet been found in the Miocene Calvert, Choptank, St. Marys, or Eastover Formations, or in the late Pliocene Chowan River Formation, all of the Chesapeake Group (Table 1). The occurrence of the Rice's Pit bowhead whale in the upper Yorktown Formation, however, establishes proof that bowhead whales inhabited the waters off eastern North America during middle Pliocene times.

FIGURE 1.—Rice's Pit, Hampton, Virginia. (W.M. Rice photo.)

study during the summers of 1972 and 1974; to the late William M. Rice for his cooperation in the removal of the specimen from his borrow pit and for his generous donation of the specimen to the National Museum of Natural History; to Gerald H. Johnson of the Department of Geology, College of William and Mary, for his time and assistance with writing the manuscript; to David J. Bohaska for his help in preparing the manuscript for publication, and especially for his advice in orienting and labeling the ear ossicles; to Samuel A. McLeod for a helpful review of the manuscript; to the late Robert McKinney of the United States Geological Survey, who photographed all of the bones except the ear ossicles, which were taken by Victor Krantz; to the members of the Department of Paleobiology, Smithsonian Institution, who put up with the inconveniences a specimen of this size creates; and to each person who aided in the tedious job of typing the various stages of the manuscript.

Thanks must also be given to Clayton E. Ray of the Department of Paleobiology, Smithsonian Institution, who acted as Westgate's advisor during the two summers in which he was a participant in the Research Intern Program.

GEOLOGIC SETTING

Rice's Pit, which is about 13.2 m (43.5 ft.) deep, is located on the Hampton Flat and is excavated into the Yorktown and overlying Tabb Formations. The Tabb Formation is composed of a fining upward sequence with a basal thin pebble sand that grades upward into a well-sorted, light gray, quartzose sand and into a surficial heterogeneous mixture of clay, silt, and fine sand. It is about 1.7 m (5.6 ft.) thick on the eastern side of the pit. The Tabb was deposited in an ancestral Chesapeake Bay during the late Pleistocene.

The Yorktown Formation exposed in Rice's Pit is a fully marine sequence that coarsens and becomes more carbonate-rich upward. At the base of Rice's Pit, the Yorktown is a sparsely fossiliferous, quartzose, clayey, fine sandy silt with less than 20% carbonate. It grades to a moderately fossiliferous, massive-bedded, fine to medium sand near the top of the formation. The uppermost 20–110 cm (0.6–3.3 ft.) is leached and partially oxidized to a soft, slightly compressive, clayey and silty fine sand.

The stratum from which the whale was removed is a medium gray, silty fine sand. The dominant minerals are quartz (56%), aragonite and calcite (41% collectively), and small amounts of glauconite, heavy minerals, and mica.

The associated fauna contains a diverse assemblage of bivalves, gastropods, and echinoderms. Barnacles, bryozoans, corals, endolithic sponges, and inarticulate brachiopods are common to rare. Foraminifers and ostracodes (Hazel, 1971) are abundant and moderately diverse. The dead right whale came to rest on the floor of a shallow shelf swept by gentle currents (Figure 2).

STRATIGRAPHIC POSITION

TABLE 1

The age assignment and stratigraphic framework of the Yorktown Formation has changed with time. Lyell (1845), Rogers (1881), Clark and Miller (1912), Mansfield (1944), and others until the early 1970s assigned a Miocene age to the Yorktown. Subsequently, it was placed in the Pliocene on the basis of the foraminiferal (Akers, 1972; Berggren, 1973), ostracode (Hazel, 1971), and molluscan assemblages (Ward and Blackwelder, 1980; Campbell, 1993). The whale came from

FIGURE 2.—Mandible of USNM 22553 during excavation in Rice's Pit. (F.C. Whitmore photo.)

the *Turritella alticostata* Zone (Zone 2) of Mansfield (1944), the *Orionina vaughani* zone of Hazel (1971), the molluscan M-5 Zone of Blackwelder (1981), and planktonic Zone N19 of Blow (1969) (Akers, 1972).

The stratigraphic placement of the whale-bearing unit within the Yorktown is somewhat problematic because of the great lateral variation in thickness and lithology of late Tertiary formations in southeastern Virginia. These changes resulted from syn- and postdepositional deformation in the terrace zone of the Chesapeake Bay impact structure on the York-James penin-

sula (G.H. Johnson, pers. comm., 1997). Rice's Pit is in a gently tilted, erosionally truncated fault block in the outer terrace zone of the Chesapeake Bay impact structure. The whale-bearing bed is probably equivalent to the middle upper Yorktown: the silty fine sand facies of Johnson (1969, 1976) and the Morgarts Beach Member of Ward and Blackwelder (1980). The sequence of beds in Rice's Pit spans the boundary between the Rushmere and Morgarts Beach Members of the Yorktown Formation, according to Campbell (1993).

Systematics

Balaena ricei, new species

TYPE SPECIMEN.—USNM 22553. Right maxilla, vomer, dorsal half of cranium, right periotic with auditory ossicles, right and left mandibles both lacking posterior ends, seven cervical vertebrae, three partial thoracic vertebrae, two lumbar vertebrae, 16 caudal vertebrae, 10 chevron bones (haemal arches), sternum, right scapula, right humerus, right radius, right ulna, four metacarpals, and eight ribs. Collected by Frank C. Whit-

TABLE 1.—Stratigraphic setting of Rice's Pit, Hampton, Virginia.

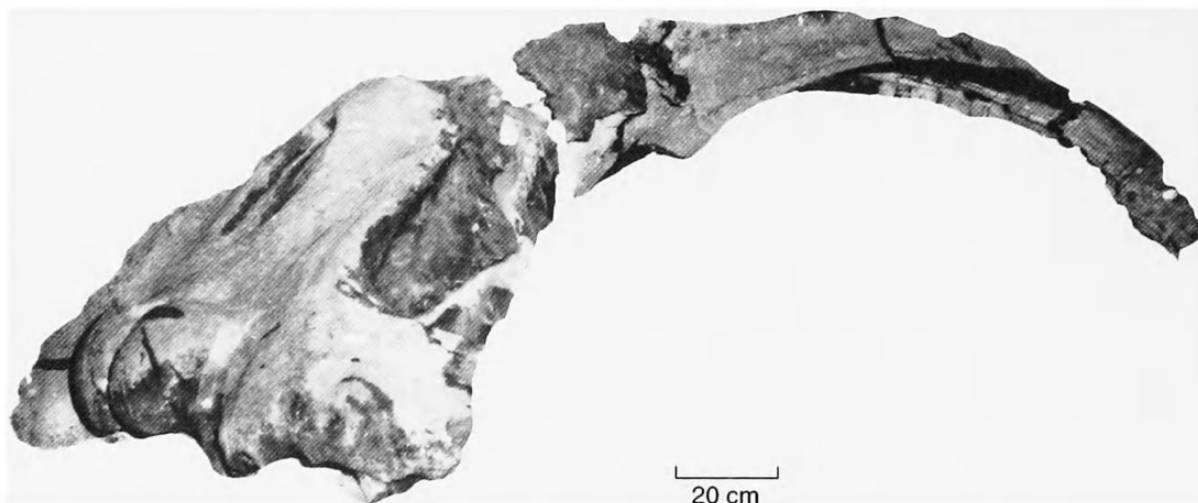| EPOCH	FORMATION	MEMBER	SECTION AT RICE'S PIT
Pleistocene	Tabb		Tabb Formation
Pliocene	Chowan River		
	Yorktown	Moore House	
		Mogarts Beach	
		Rushmere	
		Sunken Meadow	

FIGURE 3.—Skull, right posterolateral view.

more, Jr., Nicholas Hotton III, Kurt Hausschildt, and party, September 1960. Donated by William M. Rice.

ETYMOLOGY.—Named after William M. Rice, owner of the borrow pit from which the type specimen was collected.

DIAGNOSIS.—A species of *Balaena* that differs from *B. mysticetus* in having humerus longer relative to length of forearm, in having transverse processes present on first 11 caudal vertebrae, in having foramina piercing the transverse processes only in caudal vertebrae posterior to the fourth caudal, having an opening in the atlas shaped like a figure eight—the upper half for the spinal cord and the lower half for the odontoid process

FIGURE 4.—Cranium, posterior view.

of the axis; differs from *B. etrusca* in having figure-eight-shaped opening in atlas, and in smaller size; differs from *B. montalionis* in shape of supraoccipital shield.

DESCRIPTION (all measurement in centimeters unless otherwise noted).—*Cranium* (Figures 3, 4): Distance from dorsal edge of foramen magnum to anterior border of supraoccipital, 67.0; breadth of supraoccipital at temporal fossa, 78.0; dorsoventral height of occipital condyle, 25.0; breadth of occipital condyle, 15.5; height of foramen magnum, 13.0; breadth of foramen magnum, 8.5.

The lateral surfaces of the cranium are too broken to allow the delineation of the parietal bones, and the extent of the frontal bone cannot be determined because only the base of the right supraorbital process has been preserved.

The supraoccipital extends upward at approximately a 75° angle. Near the apex of the supraoccipital is a wide, laterally sloping medial ridge. Posteroventrally, this ridge is abruptly replaced by a 4 cm deep, U-shaped depression that has a prominent lateral ridge on each side. These lateral ridges gradually diminish posteroventrally for 20 cm. At this point the supraoccipital possesses no relief in the midsection. Another prominent ridge, typically found in modern balaenids, forms the lateral border of the supraoccipital along the temporal fossa. This ridge is created by upward curvature of the overhanging border of the occipital shield.

Only the base of the squamosal bone is preserved. The 35 cm section present extends anterolaterally from the supraoccipital at a 60° degree angle. The entire ventral surface of the cranium was destroyed by heavy machinery when the operator was removing fill material from the borrow pit. Fortunately, the right periotic and the associated malleus, incus, and stapes became disarticulated from the cranium, allowing close inspection of the periotic and these infrequently recovered auditory ossicles.

Maxilla (Figures 3, 5): Length, 224.0; length along curve, 240.0; breadth at nasal region, 20.0; breadth at anterior end, 10.0; height at nasal region, 32.0; height at anterior end, 0.2.
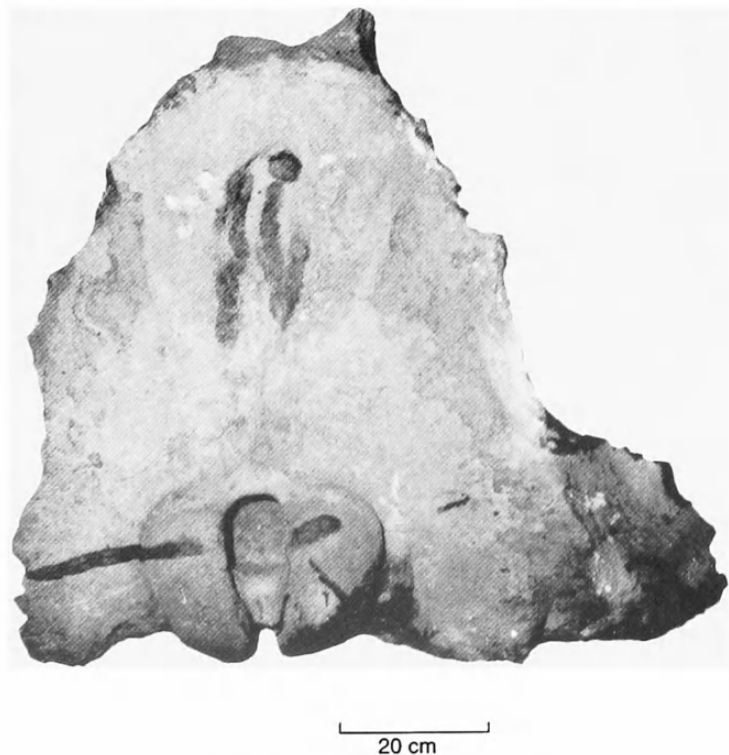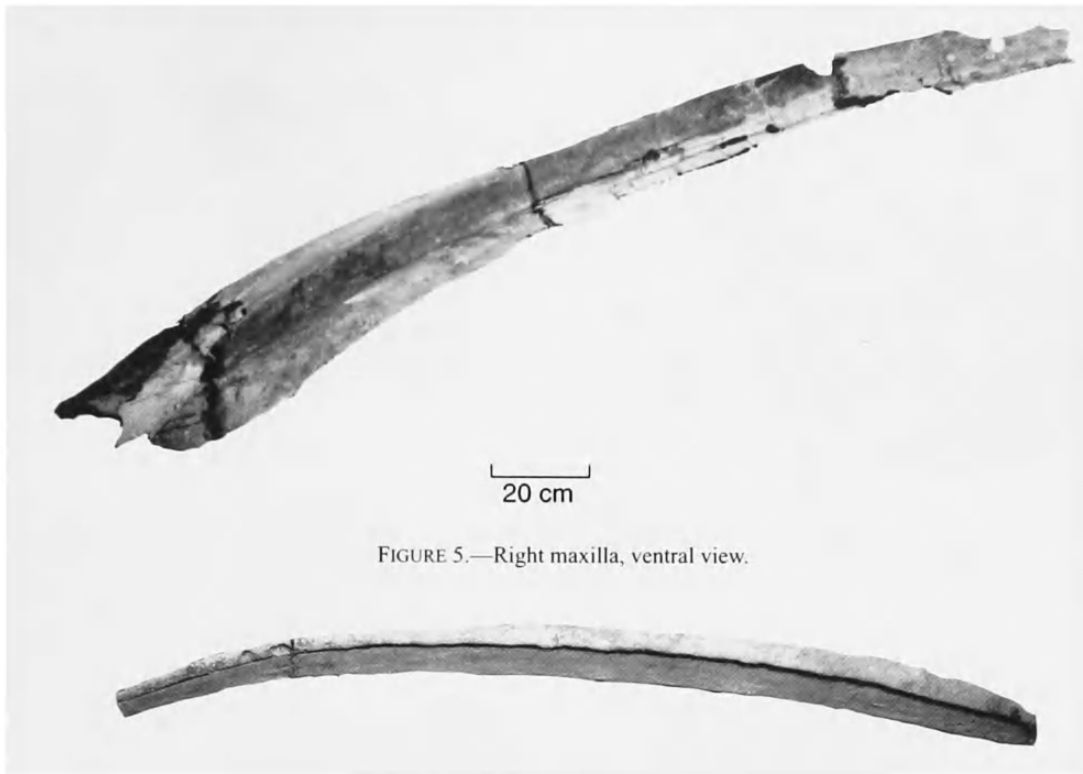
20 cm
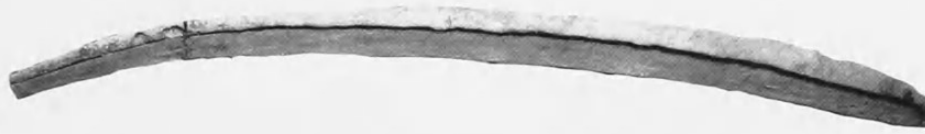
FIGURE 5.—Right maxilla, ventral view.

20 cm

FIGURE 6.—Vomer.

The maxilla extends forward from the anterior edge of the supraoccipital region in a well-rounded arc. The maxilla gradually loses its triangularity, flattening anteriorly into a thin and narrow but ventrally convex projection of bone. The external side is flat, having almost no lateral curvature. Four foramina lie on this side near the junction with the frontal.

The dorsal surface of the posterior part of the maxilla exhibits a prominent ridge along the external side bordered internally by a flat shelf upon which the premaxilla rests (Figure 3). On the inner margin of this shelf the maxilla curves downward, forming the lateral wall of the vomerine trough. At about one-third the length of the maxilla, the ridge converges with and displaces the shelf. The ridge gradually diminishes and disappears in the anterior mid-region of the maxilla. Therefore, the anterior two-thirds of the maxilla is characterized by a thin, ventrally curved and ventrally sloping surface.

Combined with the 75° slope of the occipital shield, the exaggerated curvature of the maxilla creates a very highly arched rostrum. The arch of the rostrum in conjunction with the long jaws forms an immense buccal cavity capable of engulfing huge volumes of marine organisms.

Vomer (Figure 6):   The vomer is a delicate V-shaped bone having a curvature comparable to that of the maxilla. At the internal vertex of the "V," the thin sides unite at about half the dorsal height, forming a thickened and sturdy interior. In cross section the vomer resembles an inverted "A," being solid from the crossbar to the apex.

Periotic (Figures 7, 8):   Viewed from the lateral aspect, the most prominent part of the periotic is the pars cochlearis. The length of the pars cochlearis is approximately twice its width. The surface between the fenestra rotunda and the pterygoid fossa is nearly flat with slight curvature near its edges and two shallow grooves on its face.

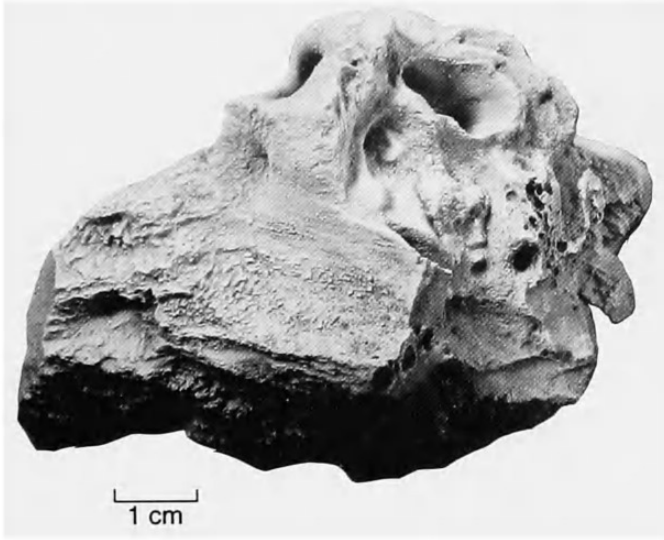1 cm

FIGURE 7.—Right periotic, ventral or tympanic view.

FIGURE 8 (left).—Right periotic, internal or cranial view.

FIGURE 9 (below).—Right malleus: *a,* dorsal view; *b,* ventral view; *c,* medial view; *d,* lateral view; *e,* anterior view; *f,* posterior view. (ant.p.=broken base of anterior process; he.f.=hemicircular facet; ho.f.=horizontal facet; p.mus.=processus muscularis.)

FIGURE 11 (right).—Right stapes: *a*, medial view; *b*, ventral view, showing articulation for incus.
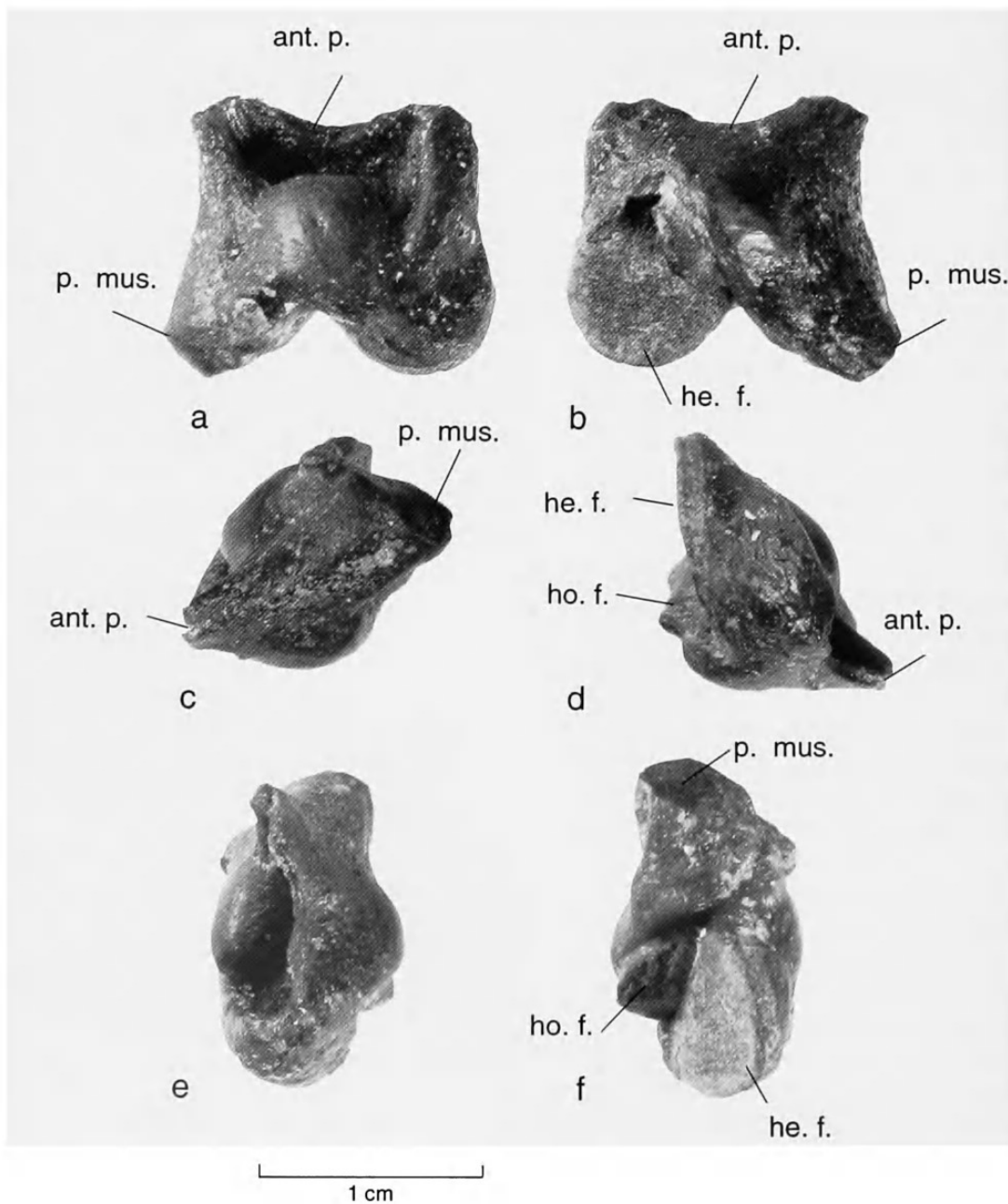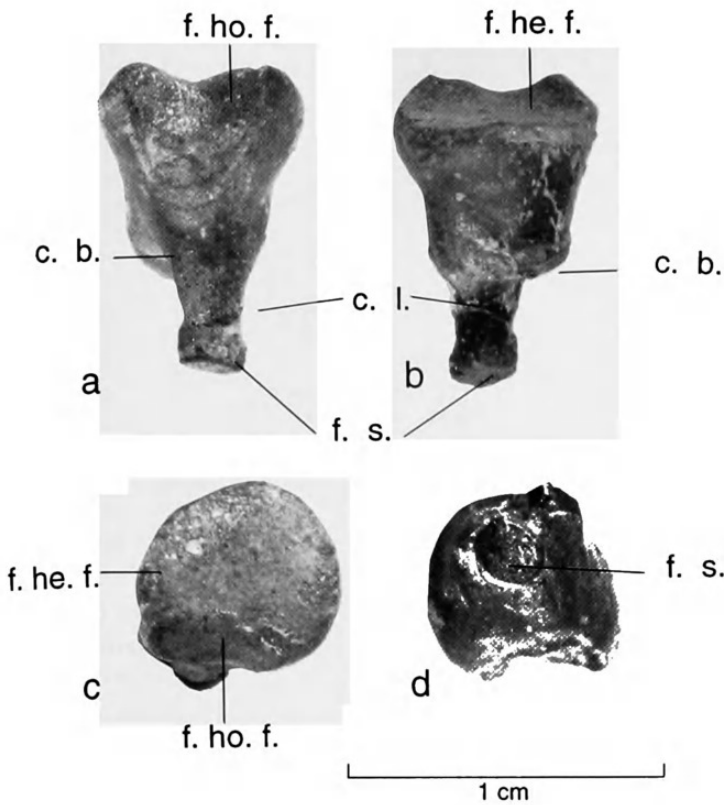

FIGURE 10.—Right incus: *a*, view showing facet for horizontal facet of malleus, and crus longum; *b*, view showing facet for hemicircular facet of malleus; *c*, view showing articular facets for malleus; *d*, view showing articular facet for stapes. (c.l.=crus longum; c.b.=crus breve (broken); f.he.f.=facet for hemicircular facet of malleus; f.ho.f.=facet for horizontal facet of malleus; f.s. =facet for stapes.)

The groove for the facial nerve and the fallopian aqueduct forms a wide channel that begins at the base of the posterior process and curves forward below and just beyond the fenestra ovalis. The fenestra ovalis is blocked by the foot plate of the stapes, which cannot be removed without damage to it. The anterior process is nearly flat, with very slight grooves radiating from its base. Only the base of the posterior process remains.

Malleus (Figure 9): Length, 19 mm; width, 16 mm. The delicate anterior process is broken, but its structure is still discernible through inspection of the cross section of the process at the point of fracture. It is apparent that the anterior process had an interior flat-bottomed groove and a rounded exterior. Posteriorly, the minutely convex hemicircular facet and the sig-

nificantly smaller horizontal facet, which join at nearly a right angle, form the contact for the incus.

Incus (Figure 10): Length, 12 mm; width, 9 mm. The two facets of the incus that are adjacent to the malleus are both concave, the smaller much more so than the other. The horseshoe-shaped larger facet meets the smaller facet at an acute angle adjacent to the cleft of the larger facet. The crus breve is missing, but the crus longum is complete. The crus longum is thin and short. At its end is a small circular facet that serves as the point of contact between the incus and the stapes.

Stapes (Figure 11): The facet on the head of the stapes and adjacent to the incus is larger and more nearly oval than that of the crus longum of the incus. The foot plate of the stapes cannot be removed from the fenestra ovalis of the periotic. The midsection of the stapes was destroyed with the breaking of the stapes head from the main body of the stapes.

Mandible: Length (partial), 310.0; length along curve (partial), 340.0; height (anterior), 35.5; height (posterior), 10.0; width (posterior), 20; width (anterior), 11.

The posterior sections of the mandibles are absent (Figures 12–14). Although the most diagnostic part of the mandible is missing, the remaining part can be informative.

The following section refers to the right mandible only. Throughout most of its preserved three meters, the mandible projects in a straight line, curving inward only in the most anterior 60 cm. At the distal end, the mandible twists inward and slightly upward. The residual dental groove extends from ap-
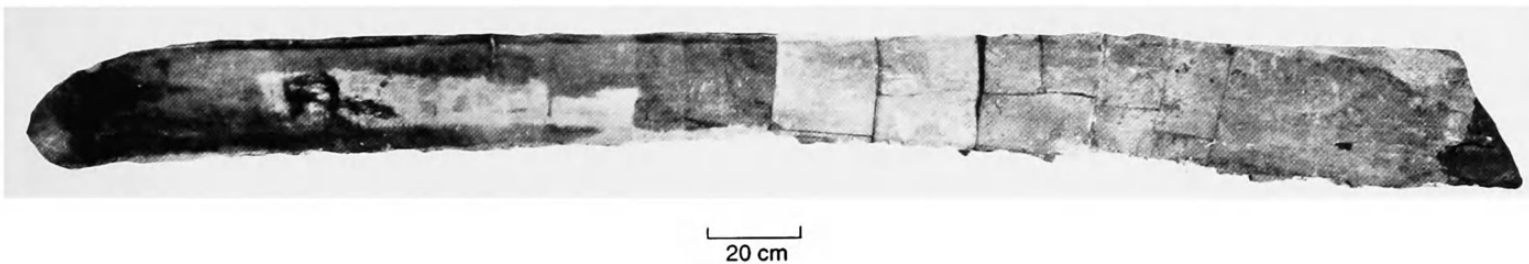

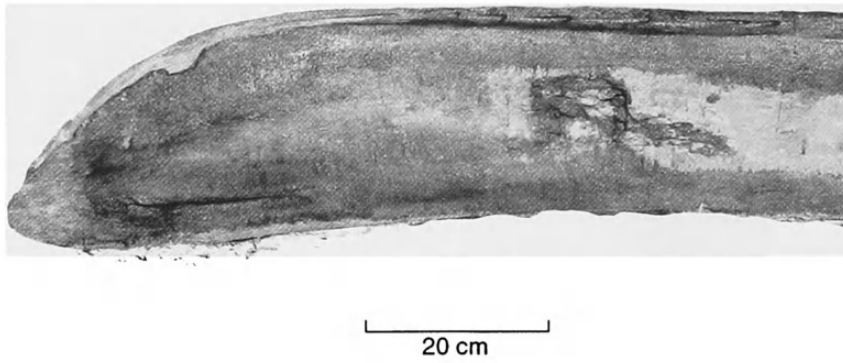FIGURE 12.—Right mandible, medial view.

FIGURE 13.—Right mandible (anterior end).

proximately the middle to the distal end of the preserved portion of the mandible, immediately below and internal to the narrow, rounded dorsal edge. From a width of 1 cm at the preserved proximal end, this groove rapidly widens to 4 cm at the anterior extremity of the jaw. The depth of the dental groove correspondingly increases from 3 cm to 5 cm. At the most proximal point, the dental groove is positioned at the midline of the mandible and is a wide notch separating two terminal projections of bone.

From the distal end of the mandible extending posteriorly along the internal face, 5 cm above the lower edge of the jaw is a broad swollen ridge, 1 cm high and 35 cm long. On the external side near the dorsal surface of the mandible are five large foramina spaced 16 to 25 cm apart along the length of the jaw. The most anterior foramen is the largest. It is the posterior end of an anteriorly directed canal that is 25 cm long, 4 cm wide, and 2 cm deep. The foramen itself is round, 1 cm in diameter; it lies 110 cm from the distal end of the mandible (measuring along the external curvature).

The height and width of the mandible increase greatly in the posterior direction. In cross section, the anterior end is small in comparison to the posterior.

Cervical Vertebrae (Figures 15–18): Transverse breadth of atlas, 54.0; vertical height of atlas, 38.0; transverse breadth of articular surface of atlas, 39.0; transverse breadth of articular surface (right facet), 16.0; vertical height of articular surface (right facet), 27.0; depth of articular concavity, 9.0; transverse

breadth of spinal canal (anteriorly), 10.5; transverse breadth of spinal canal (posteriorly), 20.0; vertical diameter of spinal canal (anteriorly), 9.5; vertical diameter of spinal canal (posteriorly), 10.0; ventral length of atlas, 12.5; ventral length of atlas with axis, 16.0; ventral length of cervical region, 26.0.

The seven cervical vertebrae are fused together, forming one compact mass. The fusion of the cervicals and the pancake-like thinness of the five posterior cervicals, both of which allow a shortening and strengthening of the neck, are characteristic of all of the balaenids. The development of this condition may be an adaptation to accommodate the intensified amount of water resistance and skull weight caused by the extreme arching of the rostrum and the heaviness of the large mandibles.

No other group of mysticetes possesses a cervical region in which all or most of the vertebrae are fused, although fusion of cervical vertebrae to a lesser extent is a common feature of many odontocetes (Eschricht and Reinhardt, 1866:107).

All of the dorsal transverse processes on the cervical vertebrae are broken. The left halves of the last five neural arches and the right half of the last neural arch in the cervical region also are broken. The remaining portions of neural arches on the
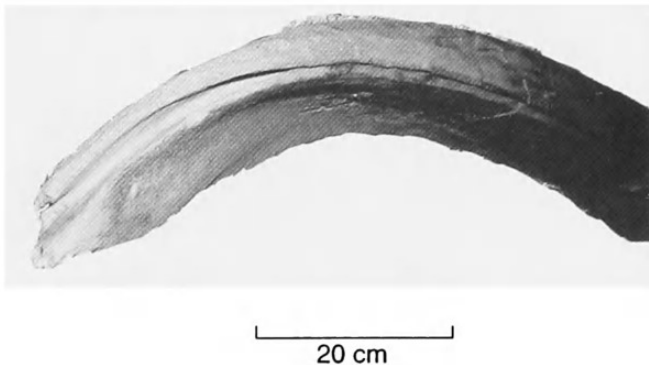

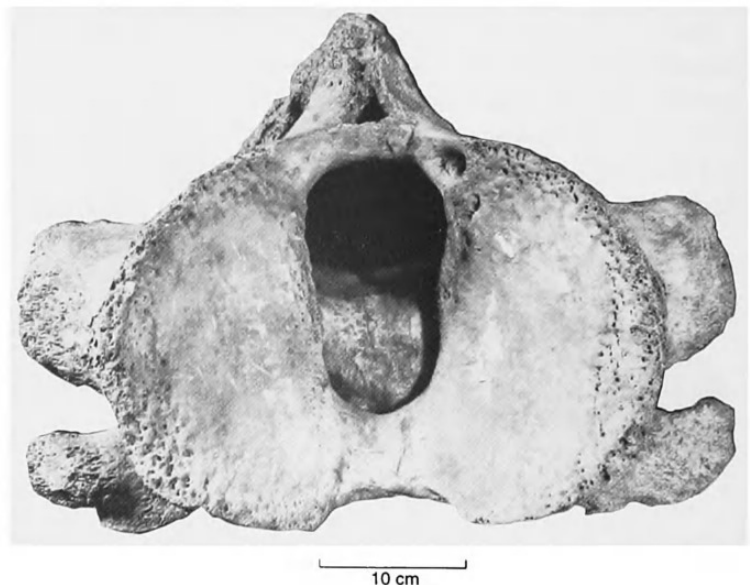FIGURE 14.—Dorsal view of anterior end of right mandible.

FIGURE 15.—Cervical vertebrae, anterior view.

FIGURE 16.—Cervical vertebrae, left lateral view.

sisting of the dorsal processes of these neural arches and the osseous growth uniting them. Of the processes on the atlas, only the dorsal process is fused to the axis. This leaves a wide gap between the atlas and axis on the lateral borders of the neural canal.

On the axis and third cervical vertebra, both ventral transverse processes are present but broken. The base of the left ventral transverse process remains on the fourth cervical and that of the right ventral transverse process on the fifth cervical. Other ventral transverse processes may once have been present, but because the surfaces of several centra are broken, their traces are absent.

The nearly flat dorsal surface of the fused centra, which is the floor of the spinal canal, is interrupted by transverse grooves that represent the lines of fusion between the vertebrae. The spinal canal changes from a subcircular opening at the atlas to an oval that is nearly twice as wide as high at the third cervical.

The second through the sixth cervical vertebrae are ventrally covered by a wide, smooth bone growth, which forms a low ridge down the midline and originates at the anterior edge of the axis (Figure 17). The lateral edges of this growth extend almost to the bases of the inferior transverse processes, where the individual vertebrae may be distinguished. This growth terminates posterior to the atlas, where a distinct transverse groove separates the ventral surface of the atlas from that of the axis.

The atlas is the largest of the seven cervical vertebrae. Its length alone constitutes almost half the length of the cervical region and, combined with the axis, forms the anterior two-thirds of the cervical region. The opening in the atlas for the spinal cord and for the odontoid process of the axis is in the shape of an inverted figure eight having a slightly constricted midsection (Figure 15). Just posterior to the dorsal margin of each articular facet of the atlas lies a bridged-over transverse arterial canal (Eschricht and Reinhardt, 1866:108). These canals are 2 cm wide and nearly 2 cm high, and they are bridged

last six cervicals are thin, wide, dorsolaterally oriented projections. They unite in an osseous mass that forms the roof of the spinal canal, which in turn is surmounted by a spinal ridge con-
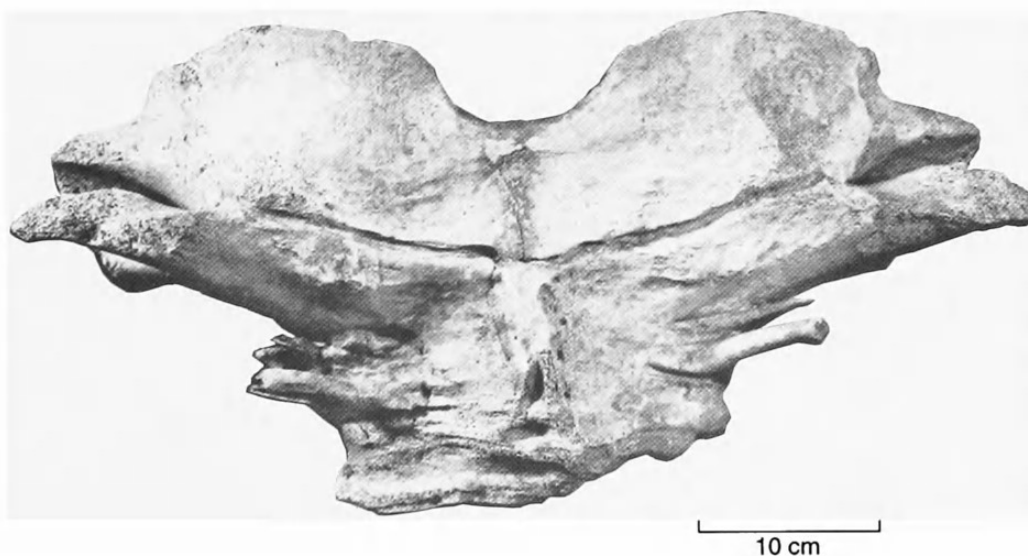

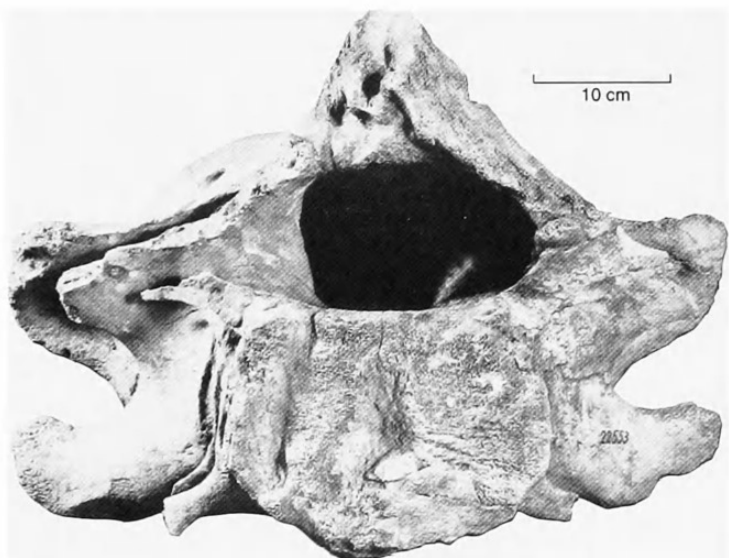FIGURE 17.—Cervical vertebrae, ventral view.

FIGURE 18.—Cervical vertebrae, posterior view.

over for a transverse distance of 5 cm on the right canal and 6 cm on the left (Figure 16). A large posteriorly directed pit 3 cm in diameter lies at the base of the dorsal process of the atlas (Figure 15). This large cavity may have been the site of cartilage that did not ossify. The transverse processes of the atlas are thick and broad, but their length cannot be ascertained because the ends are broken.

The dorsal transverse processes of the axis are much more delicate than those of the atlas (Figure 16). These axial processes are almost as wide vertically but are about one-third as thick as those of the atlas. The length is indeterminable because both processes are broken. The ventral transverse processes of the axis are approximately 16 cm long, but their ends are worn and may not be complete. An upward curvature at the ends of the ventral transverse processes and a corresponding down-

ward curvature of the dorsal transverse processes form an incomplete ring through which the vertebral artery passed (Eschricht and Reinhardt, 1866:108).

The third through seventh cervicals are almost identical in shape and dimension. All have extremely delicate transverse processes except at the point where they meet the osseous mass that is the roof of the spinal canal. The centra of these cervicals are thin and flat; each is about 1 cm thick and 16 cm high, although the seventh is thicker than its predecessors.

Thoracic Vertebrae: Three badly weathered thoracic vertebrae are present. None of these vertebrae possess fused epiphysial disks, and all are too eroded to allow accurate measurements or diagnosis.

Lumbar Vertebrae (Figures 19, 20): Only two lumbar vertebrae have been preserved. Because their exact position in the vertebral column is uncertain, the more anterior vertebra has been designated lumbar-A and the more posterior is lumbar-B. Vertical diameter of centrum (anterior), (A) 21.5, (B) 23.5; transverse diameter of centrum (anterior), (A) 24.0, (B) 26.0; anteroposterior length of centrum, (A) 15.5, (B) 17.5; height to top of dorsal process, (A) 57+, (B) 55+; transverse diameter of neural canal (anterior), (A) 12.0, (B) 9.0; vertical diameter of neural canal (anterior), (A) 7.0, (B) 5.0; transverse length of transverse processes, (A) 33+, (B) 26+.

The transverse processes of lumbar-A are longer than twice the anteroposterior length of the centrum, and they are directed slightly anteriorly. The neural spine of the vertebra is broken but is 27 cm in height and is directed posterodorsally at about a 70° angle. Neither vertebral epiphysis has fused to the centrum of lumbar-A.

The dimensions of lumbar-B are similar to those of lumbar-A, but the processes and neural canal are smaller, although the centrum is larger in diameter. The anterior epiphysis may have fused to the centrum of lumbar-B, but this is uncertain because
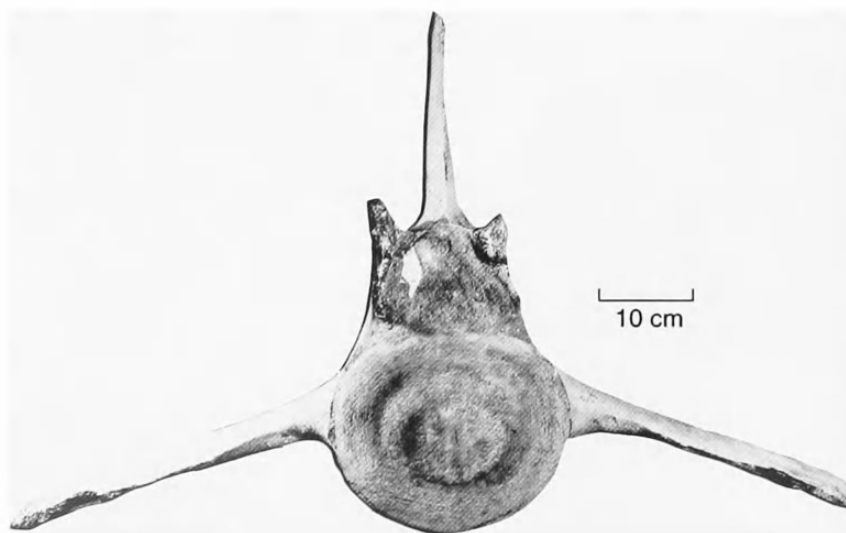

FIGURE 19.—Lumbar vertebra, anterior view.

FIGURE 20 (left).—Lumbar vertebra, right lateral view.

FIGURE 21 (right).—Fifth largest caudal vertebra, right lateral view.

10 cm

a distinct suture exists in the entire circumference between the two.

Caudal Vertebrae (Figures 21, 22, Table 2): Measurements of the first caudal vertebra (see Table 2 for others): Vertical diameter of centrum (anterior), 24.0; transverse diameter of centrum (anterior), 26.0; anteroposterior length of centrum, 20.0; height to top of dorsal process, 55+; transverse diameter of neural canal, 8.5; vertical diameter of neural canal (anterior), 5.0; transverse length of transverse processes, 24+.

The first caudal vertebra is herein defined as the most anterior vertebra possessing a contact with a chevron bone. Sixteen caudal vertebrae are present and range in length from 20 cm to 6 cm. The most anterior caudal vertebrae resemble the posterior lumbar vertebra, but these caudals have larger centra, shorter processes, and neural spines that are more vertically directed than the posterodorsally slanted spine of the posterior lumbar. Posteriorly, the vertebral processes diminish rapidly in size so that on the last eight caudal vertebrae present, no transverse processes exist at all, and the 11th caudal present is the last vertebra possessing a neural arch. The first foramina in the transverse processes appear in the sixth caudal vertebra. The foramen on the right transverse process of this vertebra measures more than twice the diameter of the foramen on the left transverse process. On the ventral surface of the caudals, the articular facets for the haemal arches turn increasingly inward on the more posterior vertebrae. By the ninth caudal these facets join to make two foramina, each 3 cm in diameter. Between these ventral foramina and those of the transverse processes lies a broad, ventrally directed groove on the surface of the centrum. A similar groove extends from the transverse process to the reduced neural arch, where another foramen has formed allowing passage transversely into the neural canal through the sides of the neural arch. Posteriorly, the grooves on the centra gradually become bridged over by bone, and the foramina lengthen into tunnel-like structures. In the 13th caudal present, which is devoid of processes, the tunnel structures are intercon-

TABLE 2.—Caudal vertebrae of *Balaena ricei* (measurements in cm).

Measurement	Caudal vertebral number														
	2	3	4	5	6	7	8	9	10	11	12	13	14	15	16
Vertical diameter of centrum (anterior)	24.5	25.0	26.0	26.0	26.0	26.0	27.0	26.5	26.0	25.5	24.5	19.0	19.0	11.5	9.0
Transverse diameter of centrum (anterior)	27.0	27.5	28.0	28.0	29.0	28.0	29.5	28.0	27.0	25.5	28.0	21.0	18.0	12.5	9.5
Anteroposterior length of centrum	18.0	22.0	21.5	19.5	20.0	19.5	20.0	19.0	18.5	18.0	17.5	12.5	10.5	8.0	6.0
Height to top of dorasl process	54.0	53+	52.0	49+	45+	43+	41+	39.0	35.0	33.5	29+	21.0	17.0	12.0	9.0
Transverse length of transverse length	22.5	20.5	17+	12.5	10.0	6.0	5+	2+	–	–	–	–	–	–	–

FIGURE 22 (left).—Eighth largest caudal vertebra, right lateral view.

FIGURE 23 (right).—Largest chevron bone, anterior view.

10 cm

10 cm

and the external curvature is about 170 cm. The distal end is nearly flat, 13 cm wide, and 4 cm thick. The most distal surface is flat to allow articulation with the sternum.

Scapula: Height (glenoid fossa to middle of convex margin), 69.0; greatest anteroposterior length, 86.0; smallest anteroposterior length (at neck), 23.0; glenoid fossa (anteroposterior length), 25.0; glenoid fossa (transverse breadth), 22.0; acromion length (ventral surface), 19.0; coracoid length (dorsal surface), 11 .0.

The presence of the prominent coracoid process on the scapula (Figures 26, 32) of *Balaena ricei* is similar to that of the scapula of *B. mysticetus* and unlike that of *Eubalaena glacialis,* which lacks the coracoid process (True, 1904). The 7 cm high coracoid process of *B. ricei* extends anteriorly for 10 cm with a slight upward and outward orientation. This process is stout, is

nected, completely encircling the centrum, and are exposed exteriorly only through five moderately sized foramina.

Haemal Arches (Figure 23): The chevrons decrease in height from 24 cm in the anteriormost to 10 cm in the posteriormost. Only slight morphological variation exists between the individual chevrons. The intermediate chevrons gradually decrease in size posteriorly, and the smallest have not fused at their vertices. The largest chevrons possess a ventral process but the smallest consist of only an arch.

Sternum: Anteroposterior length, 30.0; transverse breadth, 23.0; thickness, 5.0. Sterna of Balaenidae are characteristically variable (True, 1904). The sternum of *Balaena ricei* is shaped like an elongated, flat shield (Figure 24). The external surface is convex transversely, giving the appearance of having a low ridge along the midline. Longitudinally, the internal surface is nearly flat with a broad depression at the anterior end. Collectively, these features produce an anteroposterior cross section that is relatively thin anteriorly and posteriorly but thick in the midsection. On the lateral edges of this thickened section is a rough surface indicative of the presence of cartilage. This surface served as the point of articulation for the first pair of ribs.

Ribs (Figure 25): Only one rib remains complete. This also is the only rib with an articulating tubercular process, and it probably belongs to the first pair. The tubercular process is 12 cm long with a flat end indicative of a point of articulation. The distance from the tubercular process to the distal end is 109 cm,
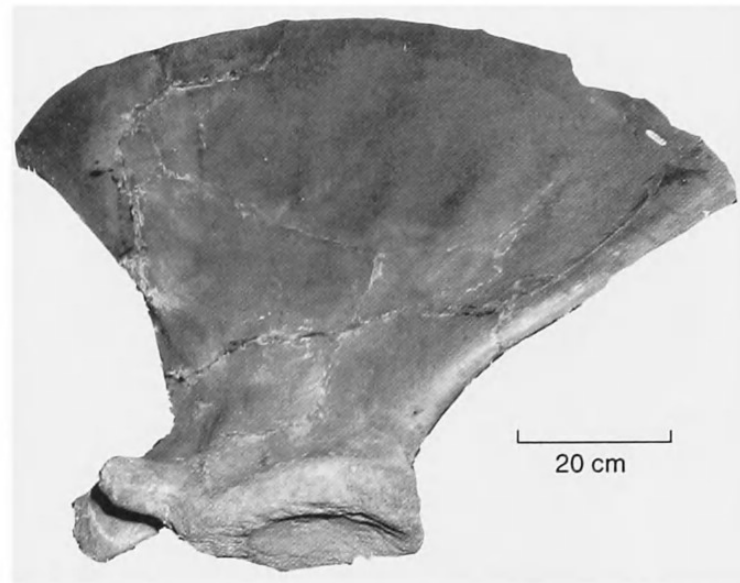

10 cm

FIGURE 24.—Sternum, dorsal view.

FIGURE 25 (left).—Right first rib, posterior view.

FIGURE 26 (right).—Right scapula, lateral view.

ovate in cross section, and has a width more than one-half its height.

The acromion process is larger than the coracoid process, but proportionately it is not as sturdy. The acromion curves internoventrally for 21 cm from its origin above the coracoid process to the acromion's anterior end. At this point the acromion is parallel to the coracoid process. The spina scapulae extends as a sharp ridge from the dorsal midsection of the acromion process to the external anterior edge of the scapula, meeting it at mid-height. The anterior edge of the scapula is 4 cm wide and shallowly convex at this point.

The anteroposterior length of the scapula is 20% greater than its height. The breadth of the neck is about 27% of the maximum anteroposterior length of the scapula. The neck of the scapula of *B. ricei* is thus more robust than that of *B. mysticetus,* which possesses a scapular neck having a breadth only about 21% of the convex margin (Eschricht and Reinhardt, 1866).

The posterior edge of the scapula is rounded and about 3 cm thick. The glenoid fossa is elliptical in circumference and shallowly concave at the center where the head of the humerus articulates with it.

Humerus (Figures 27, 28, 32):   Length, 48.5; greatest transverse diameter (proximal), 21.5; anteroposterior diameter (proximal), 28.0; greatest transverse diameter (distal), 13.0; anteroposterior diameter (distal), 23.5; least circumference of shaft, 49.0.

The humerus is similar in design and structure to the humeri of the other mysticetes. The head of the humerus is large and rounded, tilting outward and backward to allow the maximum amount of freedom from restraint at the point of contact with the glenoid fossa of the scapula. There is a shallow groove be-

tween the head and the shaft, indicating that fusion of the proximal epiphysis was not yet complete in this specimen. The midsection of the shaft is straight and has only slight lateral curvature, whereas the anterior and posterior sides of the shaft are rounded. At its distal end, the humerus flares out, forming a broad point of contact for the radius and ulna. At this contact, the base of the humerus is V-shaped. The V forms a 130° angle, and at the vertex the humerus is 13 cm thick, transversely. Another V-shaped angle of articulation is situated at the posterior edge of the point of articulation between the ulna and the humerus. This is the contact point for the olecranon process of the ulna where it abuts the posterior edge of the distal end of the humerus. This surface forms a 140° angle with the contact for the main proximal articular face of the ulna.

Radius (Figures 29, 32):   Length, 52.0; transverse diameter (proximal), 12.0; anteroposterior diameter (proximal), 19.0; transverse diameter (distal), 10.5; anteroposterior diameter (distal), 22.5; least anteroposterior diameter of shaft, 17.5.

The radius is flatter and slightly longer than the humerus. The proximal end of the radius is thicker transversely and narrower anteroposteriorly than the distal end, which is flat and widened anteroposteriorly to accommodate the carpals. The distal ends of the ulna and radius form a broader articular surface for the carpals (45 cm) than the distal end of the humerus, which is only 26 cm wide. The anterior edge of the radius curves outward anteriorly, widening the bone considerably and flattening the edge into a comparatively thin border. The posterior edge is concave, creating a 6 cm gap internally between the midsections of the radius and ulna when these bones are articulated.

Ulna (Figures 30–32):   Length, 49.0; transverse diameter (proximal), 10.0; anteroposterior diameter (proximal), 16.0; transverse diameter (distal), 7.0; anteroposterior diameter (distal), 21.0; least anteroposterior diameter of shaft, 9.5.

The ulna is lacking its distal epiphysis but is only slightly shorter than the radius, which is complete. At the proximal end of the ulna, the olecranon process also is lacking. This process
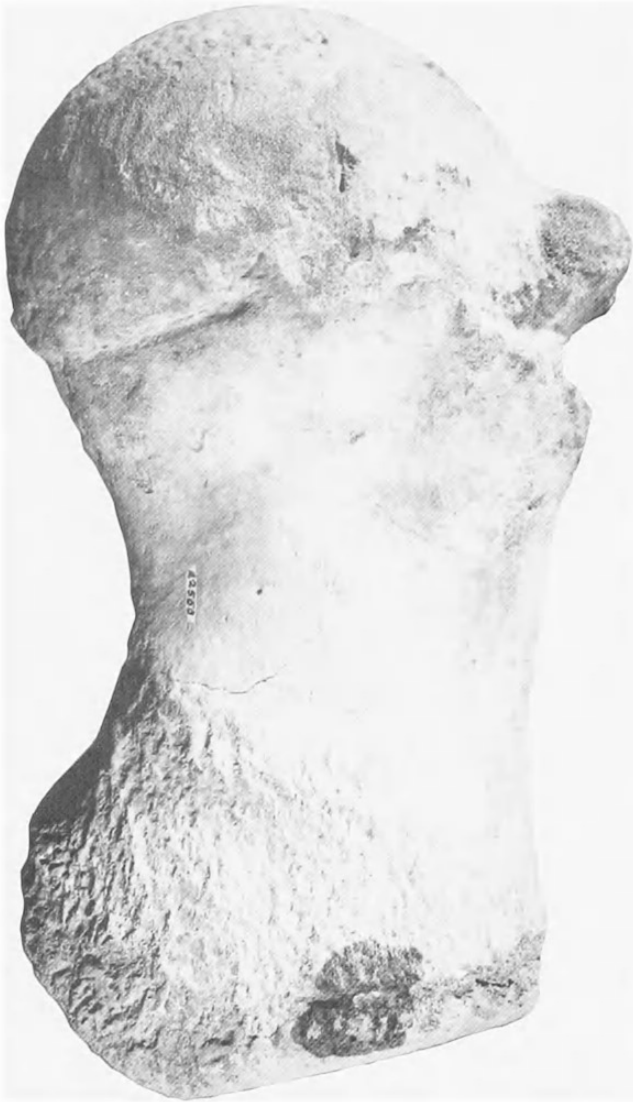
FIGURE 27.—Right humerus, lateral view.

FIGURE 28.—Right humerus, medial view.

probably had not yet fused to the main body of the ulna, but it also may not have ossified before the animal died. When the olecranon process is present, the ulna is nearly immobilized in its contact with the humerus and radius. This locking fit gives the flipper rigidity against the resistant water pressures met during swimming. As in the radius, the distal end of the ulna is flared, providing a wide carpal area of contact and creating a broader external surface toward the extremity of the flipper. The anterior edge of the ulna extends from the distal flare in a nearly straight diagonal line to the base of the proximal contact against the radius. The posterior edge is curved in a well-rounded, anteriorly directed arc.

Metacarpals (Figure 33): The only bones of the manus present are the four largest metacarpals. The metacarpals are basically similar in shape (Table 3), and size is the principal characteristic distinguishing them. Each metacarpal resembles

a flattened cylinder with a flared proximal end. All ends have the rough porous appearance that cartilage-covered bone possesses.

DISCUSSION.—This specimen closely resembles *Balaena mysticetus* but on a smaller scale. Some differences are notable, but, as many of the most advanced characteristics of *B. mysticetus* (such as the lack of a coronoid process on the mandible) have not been preserved in this specimen, a complete comparison is prevented. The mysticete flipper illustrates another struc-

TABLE 3.—Measurements of metacarpals (in cm).

Metacarpal	Length	Proximal width	Distal width	Proximal thickness
2nd	10.5	9.0	7.0	5.5
3rd	13.5	10.0	8.0	6.0
4th	9.5	10.0	7.0	5.0
5th	7.5	8.5	5.0	4.0

FIGURE 29 (left).—Right radius, lateral view.

FIGURE 30 (right).—Right ulna, medial view.

10 cm

10 cm

ture that has undergone extreme modification. The lengthening of the radius and ulna in comparison with the humerus is evidenced in most of the genera of whalebone whales, including *Balaena*. The relationship of the length of the forearm to that of the humerus in *B. mysticetus* is approximately 3 to 2, whereas in *B. ricei* it is about 1 to 1. The humerus of *B. mysticetus* has been described as "very short and thick, almost as broad as long (as 4 to 5)" (Eschricht and Reinhardt, 1866:129). That of *B. ricei* is much more elongate and narrow, the thick proximal end being only a little more than one-half as wide as the bone is long, a width-to-length ratio of about 1 to 2. In the caudal region more distinctions may be noted between *B. mysticetus* and *B. ricei*. In *B. mysticetus* the anterior caudals have very diminished traverse processes, and foramina for the branches of the

aorta may be present on the transverse processes of the second caudal (Eschricht and Reinhardt, 1866:124). In *B. ricei*, however, the transverse processes are not completely absent until the 12th caudal, and foramina on the transverse processes do not appear before the fifth caudal. A major point of distinction between *B. mysticetus* and *B. ricei* may be observed in comparing the atlas vertebrae. The atlas of *B. ricei* possesses a figure-eight-shaped opening, the upper one-half for the spinal cord and the lower half for the odontoid process of the axis (Figure 15). From an anterior view, therefore, the odontoid process is clearly visible. The atlas of *B. mysticetus* possesses no opening for the odontoid process of the axis, and from the anterior view the only visible portion of the centrum of the axis is that which is incorporated in the floor of the neural canal. The same is true of *B. etrusca* Capellini, 1873, which is much larger than *B. ricei*: its fused cervical vertebrae measure 260 mm anteroposteriorly as opposed to 166 mm for *B. ricei*.

Balaena mysticetoides Emmons, 1858, was based upon a tympanic bulla from the Yorktown Formation of North Caro-

FIGURE 31 (left).—Right ulna, lateral view.

FIGURE 32 (upper right).—Right flipper, lacking carpals and metacarpals.

FIGURE 33 (lower right).—Third right metacarpal.

lina (McLeod et al., 1993). The holotype specimen has been lost, but the figure presented by Emmons (1858, fig. 26) is of a nondiagnostic tympanic bulla of an indeterminate mysticete.

Balaena svedenborgii Lilljeborg, 1867, possesses a distinctly different caudal section from that of *B. ricei*. According to Lilljeborg, foramina do not appear in the transverse processes until the 10th caudal (fifth in *B. ricei*), and the lower channel for the branches of the aorta at the point of attachment for the haemal arches does not become a closed canal until the 15th caudal (eighth in *B. ricei;* Figure 22). McLeod et al. (1993:52) synonymized *B. svedenborgii* with *B. mysticetus*.

Balaena primigenia Van Beneden, 1872, is based upon only a posterior sphenoid, several tympanic bullae, a complete rib, and a phalanx. This species thus has no diagnostic parts comparable with *B. ricei*.

In 1852, Leidy described *B. palaeatlantica* and *B. prisca*. *Balaena palaeatlantica,* from the Miocene at City Point on the

James River in Virginia, is based upon an 8½ in. (21.6 cm) fragment of mandible, some vertebrae, and a zygomatic process. (The term Miocene as used by Leidy in 1852 includes beds that we would now designate as Pliocene.) The transverse measurements of the mandibular fragment are 2 in. (5.2 cm) anteriorly and 2¾ in. (7.0 cm) posteriorly. The height is 3¾ in. (9.5 cm) anteriorly and 4½ in. (11.4 cm) posteriorly. *Balaena prisca* is based upon a mandibular fragment 14 in. (35.5 cm) long. The vertical diameter is 3 in. (7.6 cm) and the transverse diameter, 2 in. (5.0 cm). Kellogg (1968) regarded this specimen as undiagnostic. These mandibular fragments represent species much smaller than *B. ricei,* and the holotype of *B. prisca* was considered by both Cope and Kellogg (Kellogg, 1968:125) to be from a cetothere.

Balaena simpsoni Philippi, 1887, is based upon a badly broken occipital shield, which Philippi admitted could not be accurately diagnosed. It represents an adult estimated to be 20–25 ft. (6–7.5 m) long. Donoso-Barros (1976) placed this species in the genus *Caperea*. Fordyce (1984) regarded it as undiagnostic.

Balaena affinis Owen, 1844, *B. definita* Owen, 1844, and *B. pampaea* Ameghino, 1891, are based upon tympanic bullae

TABLE 4.—Measurements of the supraoccipital shield of *Balaena montalionis* and *B. ricei* (in cm).

Measurement	*Balaena montalionis**	*Balaena ricei*
From superior margin of foramen magnum to apex of occipital shield	53.0	67.0
Width at level of superior margin of foramen magnum	66.0[†]	78.0
Width 150 mm anterior to foramen magnum	52.5	71.0
Width 300 mm anterior to foramen magnum	43.0	67.5
Width 400 mm anterior to foramen magnum	30.5	56.6

* Measurements from Capellini (1904).

[†] This measurement erroneously given by Capellini as 0.066 m.

and thus cannot be compared with *B. ricei*. *Balaena definita* is based upon a balaenopterid bulla (McLeod et al., 1993).

Balaena montalionis Capellini, 1904, from the Pliocene of Tuscany is based upon a partial skull including a complete occipital shield, squamosals, left supraorbital process of the frontal, nasals, partial maxilla, basioccipital, and basisphenoid (Capellini, 1904, pl. 1). Capellini (1904) stated that the holotype of *B. montalionis* is too incomplete to allow comparison with other fossil balaenids of Tuscany, but that it differs markedly from *B. mysticetus* in the conformation of the supraoccipital. In this respect *B. montalionis* also differs from *B. ricei* (Table 4), a difference sufficient to differentiate the two species.

Conclusions

The cosmopolitan occurrence of *Balaena* in Pliocene time was part of the appearance of the modern whale fauna, dominated by large baleen whales, sperm whales, and the many genera of the family Delphinidae (Fordyce, 1989; Whitmore, 1994). This faunal change has been attributed to changes in ocean currents resulting from the growth of the West Antarctic ice sheet, the cutting off of warm water flowing into the Atlantic from the Mediterranean, and the rise of the Isthmus of Panama.

Late Miocene and Pliocene fossils of *Balaena* are associated in Europe and North America with remains of *Balaenula*, a smaller genus now extinct (Van Beneden, 1872; Whitmore and Kaltenbach, MS). The relationship between these two genera is on tenuous ground because of the paucity of good fossil material, as is the question of the number of species of *Balaena* that existed during the Pliocene. This number may be reduced when we know more about size range and intraspecific variation in Pliocene *Balaena;* but, considering the number of species of *Balaenoptera* in modern seas, five species of Pliocene *Balaena* may not be an unreasonable number.

Literature Cited

Akers, W.H.
 1972. Planktonic Foraminifera and Biostratigraphy of Some Neogene Formations, Northern Florida and Atlantic Coastal Plain. *Tulane Studies in Geology and Paleontology,* 9: 139 pages.

Ameghino, F.
 1891. Caracteres diagnósticos de cincuenta especies nuevas de mamíferos fósiles argentinos. *Revista Argentina de Historia Natural* (Buenos Aires), 1(3a):129–167, figs. 26–75.

Berggren, W.A.
 1973. The Pliocene Time Scale: Calibration of Planktonic Foraminiferal and Calcareous Nannofossil Zones. *Nature,* 243:391–397.

Blackwelder, B.W.
 1981. Late Cenozoic Stages and Molluscan Zones of the United States Middle Atlantic Coastal Plain. *Paleontological Society Memoir,* 2: 1–34.

Blow, W.H.
 1969. Late Middle Eocene to Recent Planktonic Foraminiferal Biostratigraphy. *In* P. Brönnimann and H.H. Renz, editors, *Proceedings of the First International Conference on Planktonic Microfossils, Geneva, 1967,* pages 199–422, plates 1–54. Leiden: E.J. Brill.

Campbell, L.D.
 1993. Pliocene Molluscs from the Yorktown and Chowan River Formations in Virginia. *Publications of the Virginia Division of Mineral Resources,* 127: 259 pages, 43 plates.

Capellini, G.
 1873. Sulla *Balaena etrusca. Memorie dell'Accademia delle Scienze dell'Instituto di Bologna,* series 3a, 3:313–331.
 1904. Balene Fosili Toscane, II: Balaena montalionis. *Memorie dell'Accademia delle Scienze dell'Instituto di Bologna,* series 6, 1:47–54.

Clark, W.B., and B.L. Miller
 1912. The Physiography and Geology of the Coastal Plain Province of Virginia. *Bulletin of the Virginia Geological Survey,* 4: 274 pages.

Donoso-Barros, R.
 1976 ("1975"). Contribución al conocimiento de los Cetaceos vivientes y fosiles del territorio de Chile. *Guyana, Zoologia,* 36:1–127. [Date on title page is 1975; actually published in 1976.]

Emmons, E.
 1858. *Report of the North Carolina Geological Survey: Agriculture of the Eastern Counties, Together with a Description of the Fossils of the Marl Beds.* 314 pages.

Eschricht, D.F., and J. Reinhardt
 1866. On the Greenland Right Whale, (*Balaena mysticetus* Linnaeus). [Publications of the] *Ray Society, London,* 1866: 150 pages, 106 plates.

Fordyce, R.E.
 1984. Evolution and Zoogeography of Cetaceans in Australia. *In* M. Archer and C. Clayton, editors, *Vertebrate Zoogeography and Evolution in Australia,* pages 929–948. Perth, Western Australia: Hesperian Press.

1989.   Origins and Evolution of Antarctic Marine Mammals. *In* J.A. Crame, editor, Origins and Evolution of the Antarctic Biota. *Geological Society* (London), *Special Publication,* 47:269–281.

Hazel, J.E.
1971.   Ostracode Biostratigraphy of the Yorktown Formation (Upper Miocene and Lower Pliocene) of Virginia and North Carolina. *U.S. Geological Survey Professional Paper,* 704: 13 pages.

Johnson, G.H.
1969.   Guidebook to the Geology of the Lower York-James Peninsula and South Bank of the James River. *Guidebook,* 1: 33 pages. Williamsburg, Virginia: Department of Geology, College of William and Mary.
1976.   Geology of the Mulberry Island, Newport News North and Hampton Quadrangles. *Virginia Division of Mineral Resources Report of Investigations,* 41: 72 pages.

Kellogg, R.
1968.   Fossil Marine Mammals from the Miocene Calvert Formation of Maryland and Virginia, Part 5: Miocene Calvert Mysticetes Described by Cope. *Bulletin of the United States National Museum,* 247:103–132, plates 46–48.

Leidy, J.
1852 ("1851").   [Description of *Balaena prisca* and *B. palaeatlantica.*] *Proceedings of the Academy of Natural Sciences of Philadelphia,* 5(12):308–309. [Date on title page is 1851; published in 1852.]

Lilljeborg, W.
1867.   *On Two Subfossil Whales Discovered in Sweden.* 48 pages, 11 plates. Uppsala: W. Schultz.

Lyell, C.
1845.   On the Miocene Tertiary Strata of Maryland, Virginia, and of North and South Carolina. *Quarterly Journal of the Geological Society of London,* 1:413–427, appendix.

Mansfield, W.C.
1944.   Stratigraphy of the Miocene of Virginia and the Miocene and Pliocene of North Carolina. *In* Julia Gardner, Mollusca from the Miocene and Lower Pliocene of Virginia and North Carolina. *U.S. Geological Survey Professional Paper,* 199-A:1–16.

McLeod, S.A., F.C. Whitmore, Jr., and L.G. Barnes
1993.   Evolutionary Relationships and Classification. *In* J.J. Burns, J.J.

Mantague, and C.J. Cowles, editors, The Bowhead Whale. *Society for Marine Mammalogy, Special Publication,* 2:45–70.

Owen, Richard
1844.   Appendix to Professor Henslow's Paper, Consisting of a Description of the Fossil Tympanic Bones Referable to Four Species of *Balaena. Proceedings of the Geological Society of London,* 4:283–286.

Philippi, R.A.
1887.   *Die Tertiären und Quartären Versteinerungen Chiles.* 266 pages, 58 plates. Leipzig: F.A. Brockhaus.

Rogers, B.
1881.   *A Reprint of Annual Reports and Other Papers on the Geology of the Virginias.* 832 pages. New York: D. Appleton & Co.

True, F.W.
1904.   Whalebone Whales of the Western North Atlantic Compared with Those Occurring in European Waters, and Some Observations on the Species of the North Pacific. *Smithsonian Contributions to Knowledge,* 33: 332 pages, 50 plates.

U.S. Geological Survey
1962.   Paleontology, Evolution [Finding of 50-foot Fossil Whale]. *In* Geological Survey Research 1962. *U.S. Geological Survey Professional Paper,* 450A:474.
1965.   Significant Finds of Vertebrate Fossils in Virginia and Florida. *In* Geological Survey Research 1965. *U.S. Geological Survey Professional Paper,* 525A:71.

Van Beneden, P.J.
1872.   Les baleines fossiles d'Anvers. *Bulletin de l'Académie Royale des Sciences, des Lettres, et des Beaux-Arts de Belgique* (Bruxelles), series 2, 34:6–20.

Ward, L.W., and B.W. Blackwelder
1980.   Stratigraphic Revision of Upper Miocene and Lower Pliocene Beds of the Chesapeake Group, Middle Atlantic Coastal Plain. *U.S. Geological Survey Bulletin,* 1482-D: 61 pages.

Whitmore, F.C., Jr.
1994.   Neogene Climate Change and the Emergence of the Modern Whale Fauna of the North Atlantic Ocean. *Proceedings of the San Diego Society of Natural History,* 29:229–238.

Whitmore, F.C., Jr., and J.A. Kaltenbach
MS.   Neogene Cetacea of the Lee Creek Phosphate Mine, North Carolina.